JOURNAL OF SOLID STATE CHEMISTRY 38, 149–157 (1981)

Tunnel and Intergrowth Structures in the Gallia-rich Gallium Titanate System

L. A. BURSILL AND G. G. STONE

School of Physics, The University of Melbourne, Parkville, 3052, Australia

Received January 11, 1980; in final form April 7, 1980

Phase analysis studies of the homologous series $Ga_4Ti_{m-4}O_{2m-2}$ by electron microscopy and diffraction reveals that $m = 5$ and 7 may occur but they are metastable, appearing only in incompletely reacted specimens. Thus $m = 9$ is the lowest stable member of the series. The observation of and structure determination of a new tetragonal tunnel structure, containing hollandite-type tunnels separated by elements of the β-gallia and rutile structure types, are also reported. The stoichiometry range $M_xGa_{10+2x}Ti_{6-2x}O_{27}$ ($M = Al_2O^{2+}$; $0.80 < x < 1.20$) is suggested for this phase, since Al^{3+} is necessary to stabilize this phase. Lattice image studies of Ga_2TiO_5 reveal that it does not have the pseudobrookite structure, as assumed by previous authors, but instead adopts the "low-temperature" Ti_3O_5 structure type.

1. Introduction

The structure of $Ga_4Ti_{21}O_{48}$ is shown in Fig. 1, which shows a projection along the short 2.96-Å axis. Over 80% of the Ga was shown to reside within columns of β-gallia-type structure as emphasized in Fig. 1 (*1*). These columns are coherently intergrown within slabs of the rutile (TiO_2) structure. Empty tunnels occur at 10.3-Å intervals along $(210)_r$ planes across which the rutile slabs are displaced by $[\frac{1}{2}\frac{1}{2}\frac{1}{2}]_r$. Electron diffraction and lattice fringe studies showed that a homologous series $Ga_4Ti_{m-4}O_{2m-2}$ ($15 < m < 23$) could be made by reacting Ga_2O_3 and TiO_2 at 1570 K for 14 days (*2*). Earlier the phase boundaries for an unknown structure had been defined (see Fig. 2 and Ref. (*3*)). This can now be identified as the homogolous series $Ga_4Ti_{m-4}O_{2m-2}$. The Ga-rich limit increases from 19% at. $GaO_{1.5}$ ($m = 21$) at 1370 K to 45 at.% ($m = 9$) at 1770 K. Similarly, the Ti-rich limit decreases from $m = 21$ at 1370 K to 8 at.% per cent ($m = 50$) at 1770 K. The Ti-rich limit is in good agreement with the electron microscopic studies (*2*, *4*).

More surprising was the observation of closely spaced $(210)_r$ planar defects having stoichiometry Ga_4TiO_8 ($m = 5$) and net displacement vactor $[0\frac{1}{2}0]_r$ (Fig. 3). These appear in both slightly doped rutile and within otherwise well-ordered $Ga_4Ti_{m-4}O_{2m-2}$ (*5*). Note that Ga_4TiO_8 may also be derived from β-gallia by the operation $(001)_\beta$ $[\frac{1}{2}0\frac{1}{2}]_\beta$ (*5*).

A review of the structural relations between β-gallia, rutile, hollandite, and other derived structure types suggested that gallium titanates with $m = 5$ or 7 are closely related to hollandite (*6*).

In this paper we first show that $m = 7$ may be prepared, which contradicts the phase diagram referred to above (*3*). We

0022-4596/81/080149-09$02.00/0

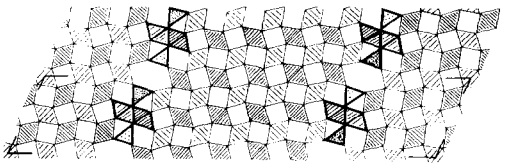

FIG. 1. Crystal structure of $Ga_4Ti_{m-4}O_{2m-2}$, $m = 25$, $[MO_6]$ octahedra share edges along the short projection axis ($c = 2.96$ Å). β-Gallia-type structure units are emphasized. Note also the empty hexagonal tunnels aligned along $(210)_r$ planes.

also give evidence that $m = 13$ may exist with hollandite and a new tunnel structure. The latter structure was determined using electron diffraction patterns, high-resolution images, and the observed orientation relationships for the three coexisting phases. However, we then show that $m = 5$ is metastable, after very long term annealing experiments, with respect to a two-phase mixture of β-gallia and an anosovite-type Ga_2TiO_5 phase at 1770 K. Similarly, $m = 7$ proved to be metastable with respect to Ga_2TiO_5 plus $m = 9$, thus confirming the published phase diagram. Replacement of some Ga^{3+} by Al^{3+} does stabilize the $m = 7$ phase and the new tunnel structure (*7*). Thus study of intermediate transitional structures by electron microscopy has led, in this case, to the preparation of a new tunnel structure in a related system.

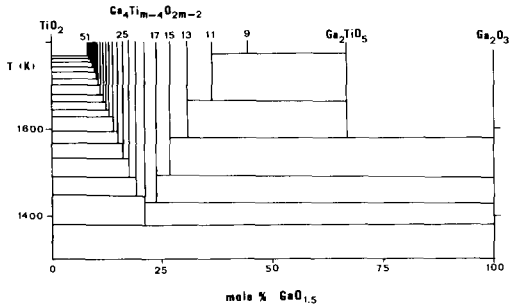

FIG. 2. TiO_2–Ga_2O_3 phase system, after Lejus *et al.* (Ref. (*3*)). The phase "*X*" may now be identified as representing the homologous series $Ga_4Ti_{m-4}O_{2m-2}$ ($9 < m < 25$).

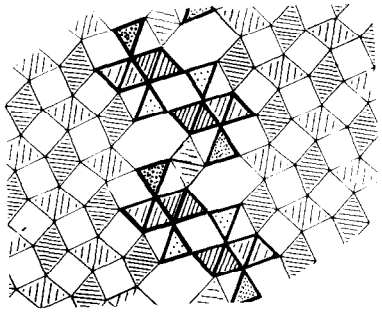

FIG. 3. Ga_4TiO_8 intergrowth defect within rutile-type structure.

2. Experimental

(*a*) *Crystal growth and preparation of samples.* Specimens $2Ga_2O_3 \cdot TiO_2$, $2Ga_2O_3 \cdot 21TiO_2$, and $2Ga_2O_3 \cdot 3TiO_2$ were made by mixing weighed amounts of finely powdered Ga_2O_3 and TiO_2 (Koch–Light, 4 *N*), pelletizing and performing a solid-state reaction in sealed platinum tubes, in air, using the experimental conditions shown in Table I. A gallia-doped rutile was made by doping a single-crystal slice from a rutile boule ($[001]_r$ orientation, National Lead Co., 99.8% purity). A Ga_2O_3 pellet was placed on top of the slice, which was then heated in an open platinum boat, in air. The pellet reacted with the rutile in toto to give a black reacted layer on top with an orange slab of rutile remaining below. Specimens

TABLE I

SPECIMEN PREPARATION CONDITIONS

Specimen	Stoichiometry	Temperature (K)	Time (days)
Gallia-doped rutile	$Ga_4Ti_{196}O_{398}$ (only Ga-rich portion was studied)	1270 + 1770	8 + 5
$2Ga_2O_3 \cdot 21TiO_2$	$Ga_4Ti_{21}O_{48}$ ($m = 25$)	1770	2
$2Ga_2O_3 \cdot TiO_2$	Ga_4TiO_8 ($m = 5$)	1770	23
$2Ga_2O_3 \cdot 3TiO_2$	$Ga_4Ti_3O_{12}$ ($m = 7$)	1720 + 1770	2 + 7

were selected from the reacted layer for this study. Further reaction did not occur after heating at 1770 K for 5 days. All specimens appeared homogeneous under an optical microscope.

Thin fracture fragments of each specimen were obtained by grinding in an agate mortar under chloroform and these were then deposited onto carbon lace support films.

(*b*) *Electron optical parameters.* A slightly modified BLG goniometer was used in a JEOL-100C electron microscope. The objective lens pole pieces had spherical aberration coefficient C_S = 2.4 mm, focal length, f_0 = 2.2 mm, and chromatic aberration coefficient C_c = 2.0 mm. Most of the micrographs were recorded using slightly defocused illumination (semicone angle 0.6–1.0 mrad) and objective lens defocus −1000 Å, when the effective point-to-point resolution is limited to 3.2–3.8 Å (*8*).

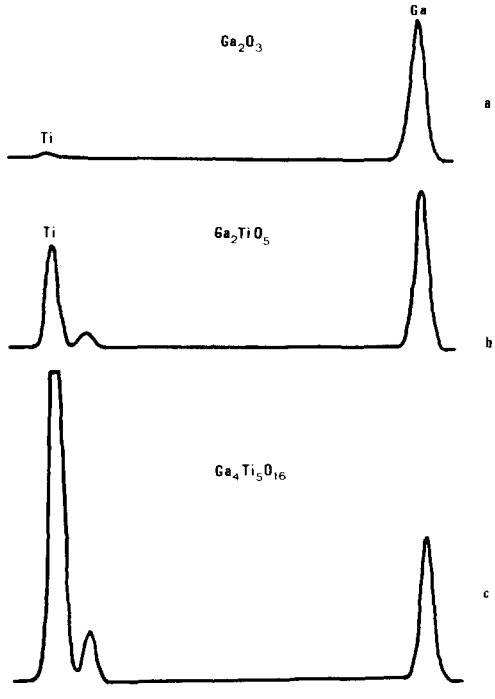

FIG. 4. XRF spectra showing characteristics of β-gallia (a), Ga_2TiO_5 (b), and $Ga_4Ti_5O_{16}$ (c).

(*c*) *Energy-dispersive X-ray fluorescence microanalysis.* Specimens $2Ga_2O_3 \cdot TiO_2$ and $2Ga_2O_3 \cdot 3TiO_2$ were also studied in a JEOL-100CX analytical electron microscope fitted with a Kevex detector. This allowed for rapid determination of the number of phases present. Both specimens were two phase: $2Ga_2O_3 \cdot TiO_2$ contained small grains (~0.1–0.5 μm) of a Ga-rich phase (Fig. 4a) plus similar grains of a phase containing both Ga and Ti (Fig. 4b) whereas $2Ga_2O_3 \cdot 3TiO_2$ showed the latter plus a Ti-rich phase (Fig. 4c). Quantitative analyses were not attempted but there were indications that this may be possible using thin fragments where fluorescence and adsorption may be negligible. The curves shown in Fig. 4 were reproduced consistently from grain to grain if small fragments were selected. Thus a calibration may be carried out using a mixed metal oxide homologous series and electron diffraction patterns if necessary.

3. Electron Microscopic Observations

(*a*) *Gallia-doped rutile.* Figure 5a shows an area of m = 7 structure containing two distinct types of planar defects parallel to $(210)_r$; these differ in the phase shift of the $Ga_4Ti_3O_{12}$ image across the defects. The corresponding diffraction pattern (Fig. 5b) was indexed using the monoclinic cell parameters a_7 = 10.3 Å, b_7 = 2.96 Å, c_7 = 7.08 Å, and β = 105.2°, which were obtained by matrix analysis of the homologous series.

Figure 6a shows an extensive area of an ordered crystal structure which gave a diffraction pattern (Fig. 6b) which indexed using the monoclinic cell parameters for m = 9, i.e., a_9 = 10.3 Å, b_9 = 2.96 Å, c_9 = 8.88 Å, and β = 103.2°. This phase was predominant but m = 7 grains occurred regularly.

(*b*) $2Ga_2O_3 \cdot 21TiO_2$. A range of $Ga_4Ti_{m-4}O_{2m-2}$ structures were found with $21 < m < 29$, as expected for a specimen having mean stoichiometry $MO_{1.92}$ (m =

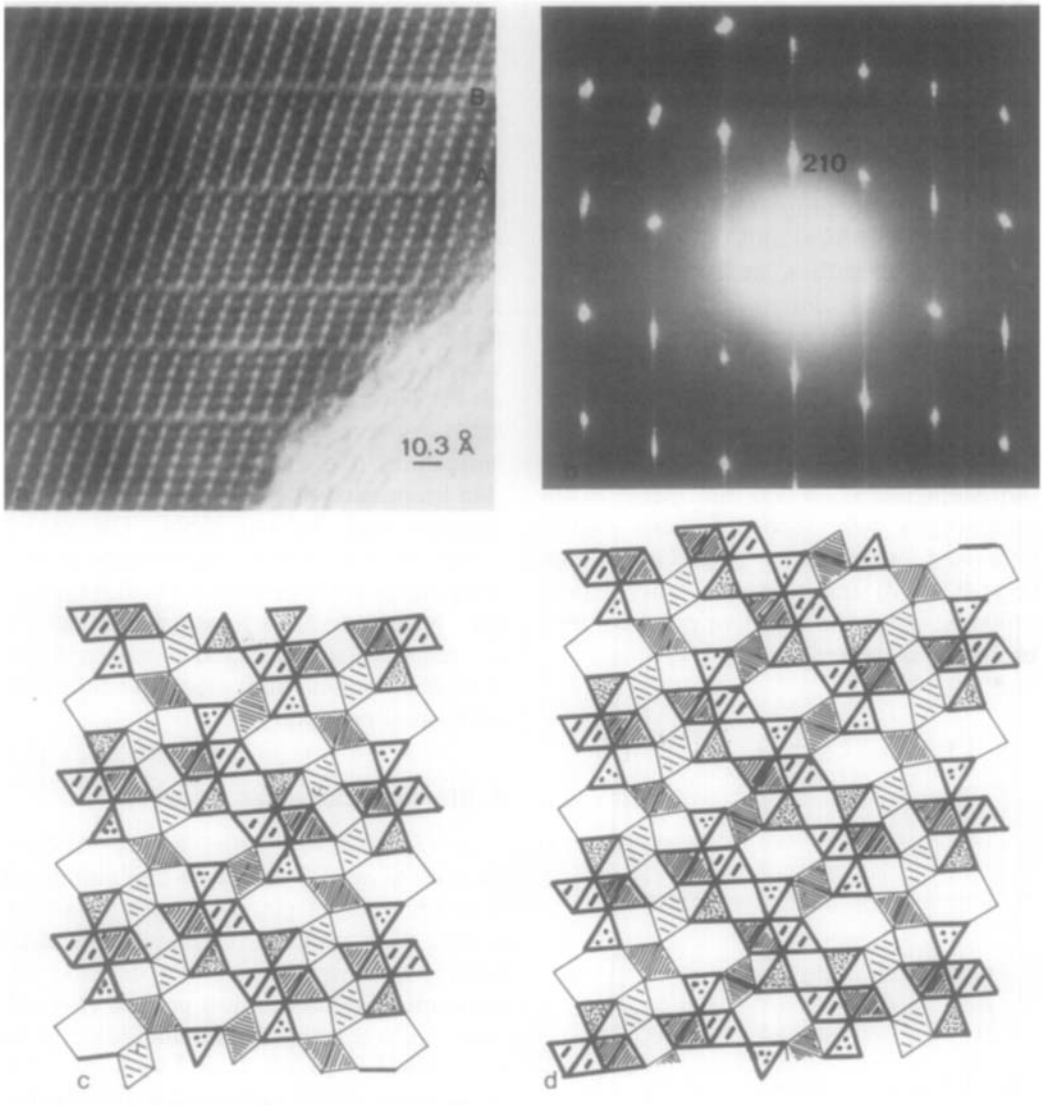

FIG. 5. (a) Intergrowth defects parallel to $(210)_r$ in $Ga_4Ti_9O_{12}$ ($m = 7$). Note the two distinct types of phase shift in the white blob image, labeled A and B. (b) Diffraction pattern corresponding to (a), showing diffuse streaks normal to intergrowth effects. (c,d) Structure of intergrowth defects, showing two and three slabs of Ge_4TiO_8 for defects labeled A and B in (a).

25). However, some crystal flakes gave complex diffraction patterns which could be resolved into three distinct reciprocal lattice nets using a small selected area aperture. Thus the complex pattern Fig. 7a was indexed using cell parameters for orthorhombic $Ga_4Ti_9O_{24}$ ($m = 13$; with $a_{13} = 10.3$ Å, $b_{13} = 2.96$ Å, $c_{13} = 12.66$ Å; see Fig. 7b); tetragonal hollandite ($a_h = 10.11$ Å, $c_h = 2.96$ Å; see Fig. 7c) and a new tetragonal net with $a_x = 12.66$ Å (see Fig. 7d). High-resolution images showed a coherent intergrowth of $m = 13$ with a single lamellar of the $a_x = 12.66$ Å structure (Fig.

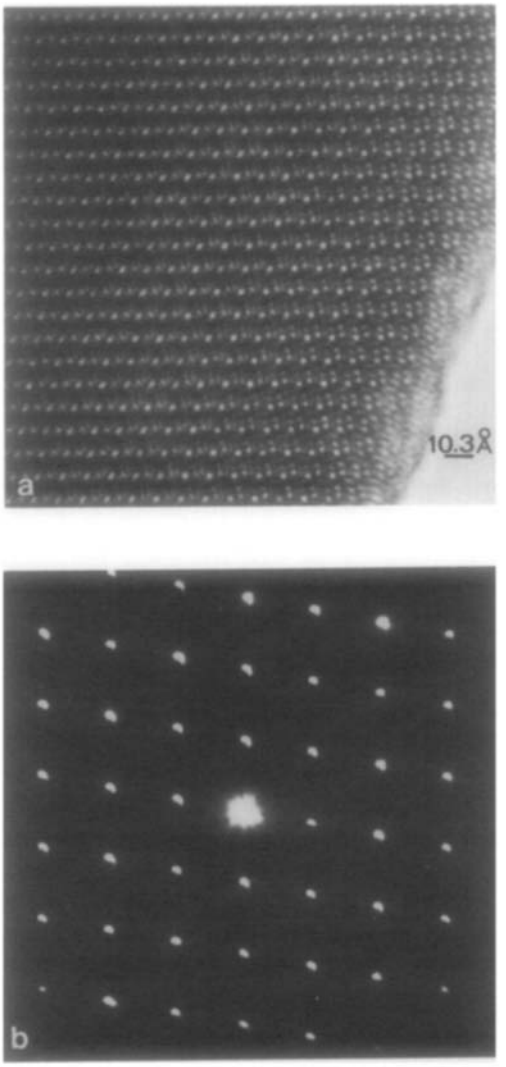

FIG. 6 (a,b) High-resolution image and corresponding diffraction pattern of $Ga_4Ti_5O_{16}$ ($m = 9$).

8a) and, nearby, an incoherent grain boundary between the hollandite phase and the new tetragonal phase (Fig. 8b).

(*c*) $2Ga_2O_3 \cdot TiO_2$. The two phases found by XRF microanalysis were identified as Ga_2TiO_5, an orthorhombic pseudobrookite-type structure according to Refs. (*2, 3*), indexed using $a_p = 9.80$ Å, $b_p = 10.00$ Å, $c_p = 3.61$ Å, and monoclinic β-gallia, indexed using $a_\beta = 12.23$ Å, $b_\beta = 3.04$ Å, $c_\beta = 5.80$ Å, and $\beta = 103.7°$ (*9*). Both phases were usually very well ordered, showing sharp diffraction spots and defect-free images (Fig. 9a).

(*d*) $2Ga_2O_3 \cdot 3TiO_2$. The Ga-rich phase was identified as Ga_2TiO_5 as above and the Ti-rich phase was indexed as $Ga_4Ti_5O_{16}$, i.e., $m = 9$, with a small fraction of $m = 11$. (Another specimen of the same stoichiometry which had been reacted at 1720 K for only 45 hr showed Ga_2TiO_5 plus a mixture of $Ga_4Ti_{m-4}O_{2m-4}$ with $19 < m < 25$ and β-Ga_2O_3 and $m = 5,7$ intergrowths. Again we found that the XRF technique led to rapid identification of these structures and rejection of this sample as incompletely reacted.)

4. Discussion

(*a*) *Intergrowth defects in* $m = 7$. The geometry of the two types of defects observed in Fig. 5a was readily deduced by assuming the white blobs in the image represent the larger empty hexagonal tunnels in the $Ga_4Ti_{m-4}O_{2m-2}$ structures. Thus the observed arrangement of blobs was reproduced by intergrowing two and three $(210)_r$ slabs of Ga_4TiO_8 ($m = 5$) within the $m = 7$ structure, as shown in Figs. 5c and d, respectively. This type of image interpretation has already been established for objective lens defocus of -1000 Å, in (*5*).

(*b*) *New tetragonal tunnel structure*. This structure was deduced by noting its coherence with $m = 13$ and its orientation with respect to the hollandite in Figs. 8a and b. The intergrowth in Fig. 8a occurs normal to the $(210)_r$ planes of $m = 13$. Figure 8c shows a model for the intergrowth whereby hexagonal tunnels at the interfaces have been converted into hollandite-type tunnels. These are linked by strips of β-gallia-type structure, leaving a small column (circled) of rutile-type structure within. The new tunnel structure generated by repeti-

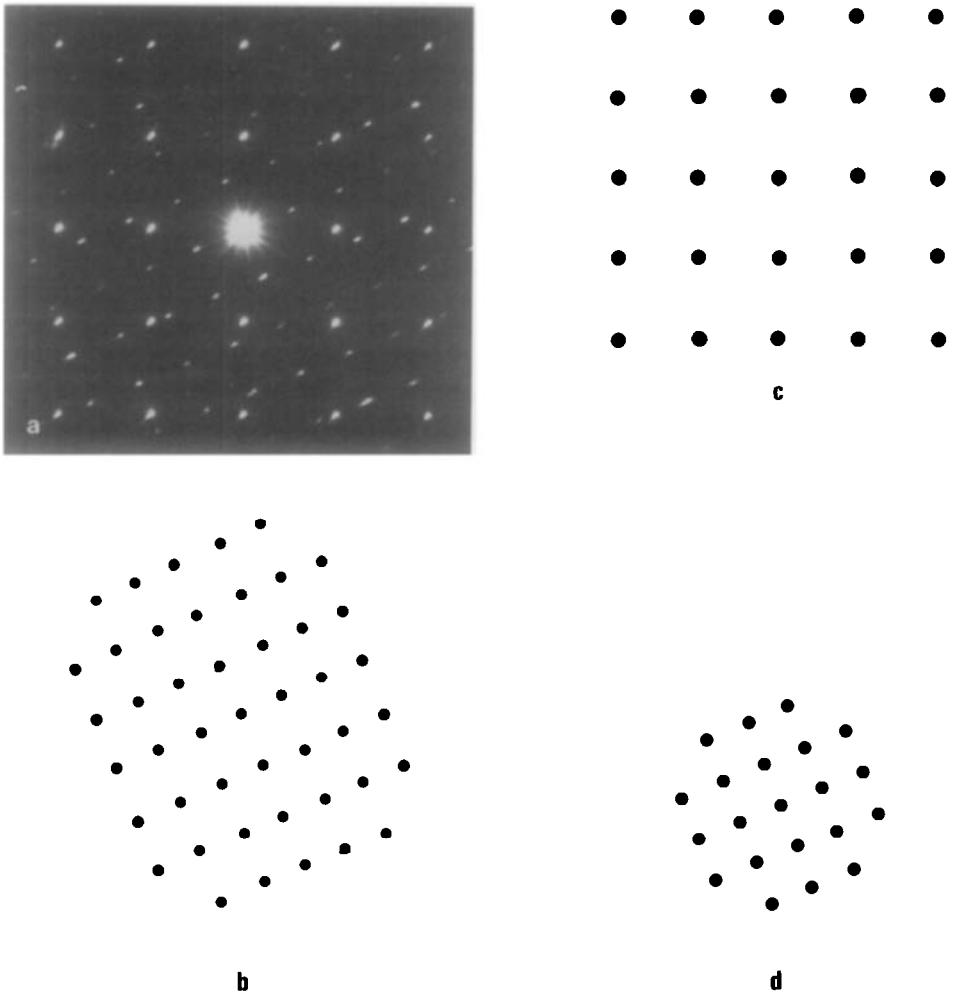

FIG. 7. (a) Electron diffraction pattern from specimen $2Ga_2O_3 \cdot 21TiO_2$ showing three reciprocal lattice nets. (b) Reciprocal lattice net for $Ga_4Ti_9O_{24}$ ($m = 13$). (c) Reciprocal lattice net for hollandite. (d) Reciprocal lattice net for new tetragonal tunnel structure having $a_x = 12.66$ Å.

tion of these units has tetragonal cell parameters $a_x = 12.66$ Å and $c_x = 2.96$ Å. If we assume M^{2+} ions occupy the tunnels as they do in hollandite we obtain the chemical formula $M_xGa_{10+2x}Ti_{6-2x}O_{27}$. Since this phase was obtained from the $2Ga_2O_3 \cdot 3TiO_2$ ($m = 7$) preparation it is not clear whether there are any ions in the tunnels. If $x = 0$ then the framework has stoichiometry $Ga_{10}Ti_6O_{27}$. On the other hand divalent (e.g., Ca^{2+}) or monovalent ($M = 2Na^+$, $2K^+$) impurities may have been inadvertently incorporated. However, attempts to prepare this phase succeeded only when the mixture contained Al_2O_3 and it would seem more likely that $M = [Al_2O]^{2+}$ with Al occupying tetrahedrally coordinated sites in the hollandite-type tunnels, as suggested in Ref. (6). This requires that oxygen also be incorporated in the tunnels, as shown in Fig. 8c. In this case the stoichiometry becomes $Al_{2x}Ga_{10+2x}$

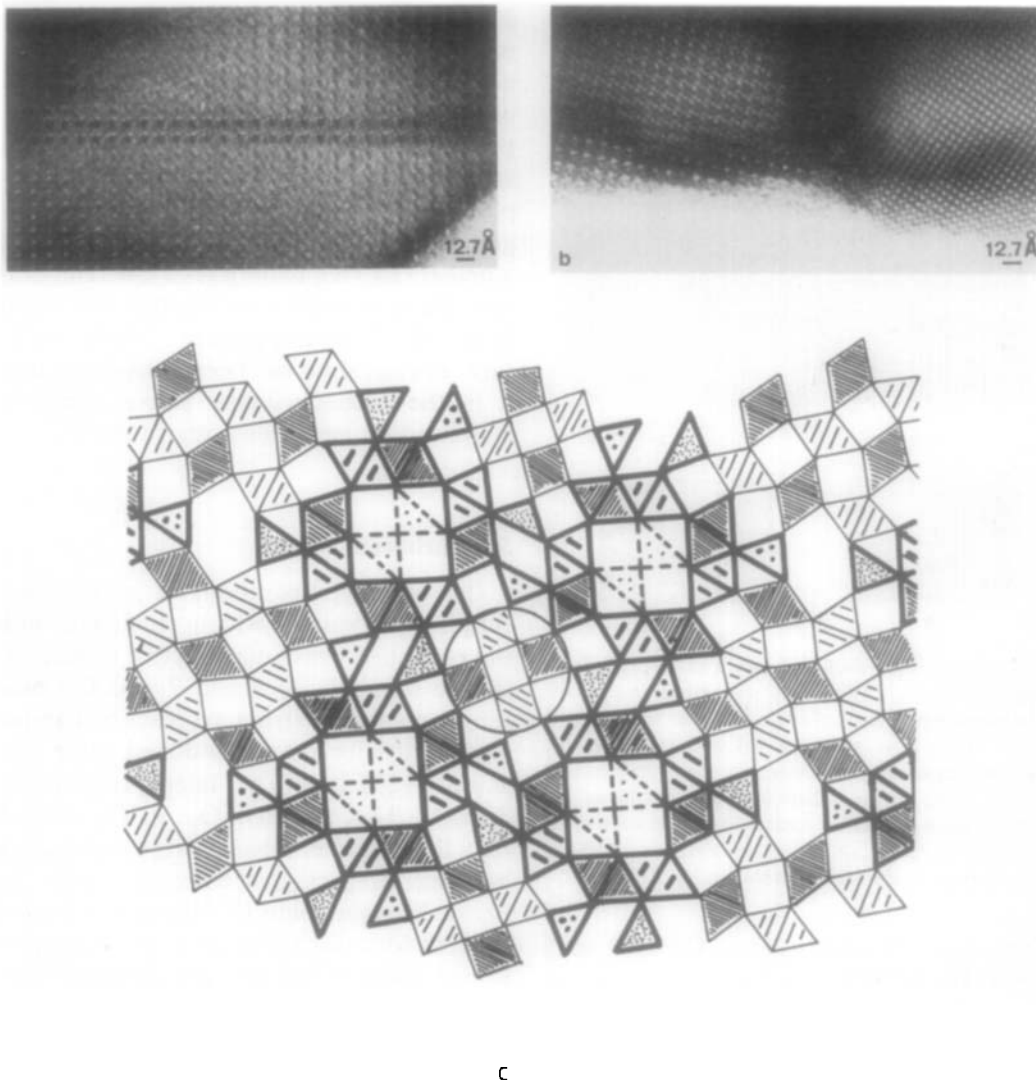

FIG. 8. (a) High-resolution image showing intergrowth of one lamellar of a_x = 12.66 Å structure within m = 13. (b) Incoherent grain boundary between hollandite phase ($M_xGa_{2x}Ti_{8-2x}O_{16}$) and new tunnel structure identified as $M_xGa_{10+2x}Ti_{6-2x}O_{27}$. (c) Structural drawing of intergrowth defect shown in (a). Note intergrowth of hollandite-type tunnels, β-gallia-type structural units linking the tunnels and surrounding a 2 × 2 column of corner-shared unit of the rutile-type structure (circled).

$Ti_{6-2x}O_{27+x}$. Crystals suitable for X-ray structure analysis are required to settle this point. For hollandite we showed that $0.8 < x < 1.2$, giving rise to apparent incommensurate superlattices along the tunnel direction (*10, 11*). It has not yet been possible to study ordering along the tunnels in the $M_xGa_{10+2x}Ti_{6-2x}O_{27}$ phase. We note that there is no obvious coherence between the latter and the hollandite phase, explaining the complex nature of the interface observed in Fig. 8b. Both the structural principles found here for $M_xGa_{10+2x}Ti_{6-2x}O_{27}$ and those recently de-

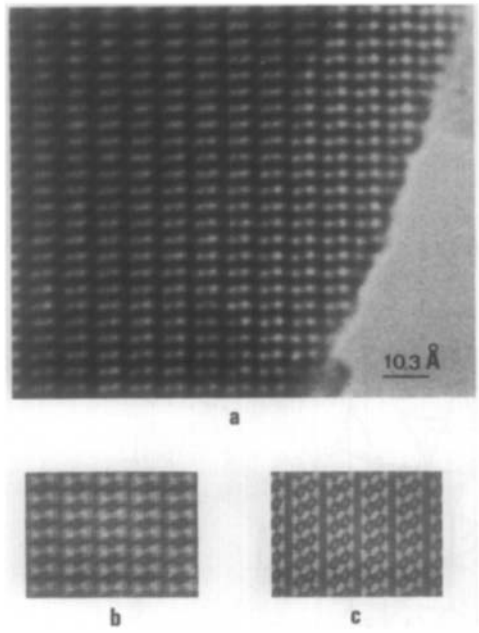

FIG. 9. (a) High-resolution image of Ga_2TiO_5 from specimen $2Ga_2O_3 \cdot TiO_2$ $[001]_p$ projection. (b,c) Computer-simulated images of orthorhombic "low-temperature" Ti_3O_5-type structure (b) and orthorhombic pseudobrookite-type structure (c). Note that (b) and (c) are easily distinguished and that (b) gives the correct match. (Electron optical parameters are crystal thickness 156 Å, objective lens defocus −1100 Å, and effective instrumental resolution 3.6 Å.)

scribed for $Ba_xGa_{10+2x}Ti_{8-2x}O_{31}$ (*12*) may readily be extended to allow the hollandite-type tunnels to be further separated by incorporating larger elements of β-gallia and rutile between the tunnels.

(*c*) *Anosovite-type Ga_2TiO_5 phase.* It has been assumed in the literature (*2, 3, 13*) that Ga_2TiO_5 has the pseudobrookite structure. However, image calculations were carried out in order to confirm this interpretation. We were surprised to find that we had to use, instead, atomic coordinates for the "low-temperature" anosovite phase reported by Åsbrink and Magneli (*14*), in an *orthorhombic* space group in order to obtain an acceptable image match. Thus Fig. 9b, showing the "low-temperature" Ti_3O_5 structure, gives good agreement whereas Fig. 9c, for Pauling's pseudobrookite structure using identical cell parameters, does not match the experimental image. It is interesting that the image can give such a positive distinction between these two structures, which differ only in small displacements of both the metal and the oxygen atoms (*14*). It is not yet clear to us whether Ga_2TiO_5 undergoes a low-temperature phase transition or whether Ga stabilizes the "low-temperature" Ti_3O_5 structure. Previously it has been considered that it is the pseudobrookite phase which is stabilized by metal ions other than Ti.

5. Conclusion

Our earlier preparations of gallia-doped rutiles gave results which conflicted with the published phase diagram (*3*); in particular we found $m = 5$ and 7 and the new tetragonal tunnel structure described above (see results for the gallia-doped rutile and $2Ga_2O_3 \cdot 21TiO_2$). The later preparations $2Ga_2O_3 \cdot TiO_2$ and $2Ga_2O_3 \cdot 3TiO_2$ showed that these earlier results were misleading and that preparations consistent with the phase diagram could be obtained provided the reactions were allowed to go to completion by using sufficiently long heating times. Thus the $m = 5$ and 7 phases proved to be metastable leaving $m = 9$ as the lower limit for m.

Attempts to prepare $M_xGa_{10+x}Ti_{6-2x}O_{27}$ as pure phases were not successful and it was assumed that this, too, was metastable. However, we have recently found that the presence of Al^{3+} stabilizes this phase (*7*). In addition a number of other hollandite-related superstructures have been found (*7*).

Stabilization of the "low-temperature" Ti_3O_5 structure type by Ga, with its almost regular ccp oxygen array, may be simply due to the relatively small ionic radius of Ga^{3+} compared with the radii of Ti^{3+} and Fe^{2+}/Fe^{3+}.

Acknowledgments

This work was supported financially by the Australian Research Grants Committee. The authors would like to thank Mr. R. Glaisher for help with the computed images.

References

1. D. J. LLOYD, I. E. GREY, AND L. A. BURSILL, *Acta Crystallogr. Sect. B* **32,** 1756 (1976).
2. R. M. GIBB AND J. S. ANDERSON, *J. Solid State Chem.* **5,** 212 (1972).
3. A. LEJUS, D. GOLDBERG, AND A. REVCOLEVSCHI, *C.R. Acad. Sci. Paris Ser. C* **263,** 1223 (1966).
4. L. A. BURSILL, *Acta Crystallogr. Sect. A* **35,** 449 (1979).
5. G. G. STONE AND L. A. BURSILL, *Phil. Mag.* **35,** 1397 (1977).
6. L. A. BURSILL, *Acta Crystallogr. Sect. B* **35,** 530 (1979).
7. L. A. BURSILL AND G. GRZINIC, paper in preparation.
8. L. A. BURSILL AND A. R. WILSON, *Acta Crystallogr. Sect. A* **33,** 672 (1977).
9. S. GELLER, *J. Chem. Phys.* **33,** 676 (1960).
10. L. A. BURSILL AND G. GRZINIC, *Acta Crystallogr. Sect. B* **36,** 2902 (1980).
11. L. A. BURSILL, *in* "Direct Imaging of Atoms in Crystals and Molecules" (Proc. Nobel Symp. 47); *Chem. Script.* **14,** 83 (1978/1979).
12. L. A. BURSILL, *Acta Crystallogr. Sect. B* **36,** 2897 (1980).
13. TH. ARMBRUSTER, *N. Jb. Miner. Mh.* 109 (1979).
14. S. ÅSBRINK AND A. MAGNELI, *Acta Crystallogr.* **12,** 575 (1959).